Performance of Fault Severity Estimation in 7-Phase Electrical Machines under Noisy Conditions

Lu Zhang, Claude Delpha, Demba Diallo

Performance of Fault Severity Estimation in 7-Phase Electrical Machines under Noisy Conditions

Lu Zhang and Claude Delpha
Université Paris Saclay, CNRS, CentraleSupélec
Laboratoire des Signaux et Systèmes
Gif sur Yvette, France
lu.zhang@centralesupelec.fr, claude.delpha@centralesupelec.fr

Demba Diallo
Université Paris Saclay, CentraleSupélec, CNRS
Group of Electrical Engineering of Paris
Gif sur Yvette, France
demba.diallo@centralesupelec.fr

2023 Prognostics and Health Management Conference (PHM) | 979-8-3503-0014-7/23/$31.00 ©2023 IEEE | DOI: 10.1109/PHM58589.2023.00053

***Abstract*—This work proposes a method for estimating fault severity in the presence of noise using the measured currents for a 7-phase electrical machine. The method is based on analytical models in stationary reference frames and analysis of the DC and fundamental components in the four fictitious machines. The slope of the decision function from the CUSUM algorithm, which will be noticeably different depending on the fault severity, is used to assess the performance of the fault severity estimation rapidly. The effects on the decision function's slope of the fault severity estimation for different noise levels are evaluated. The simulation results show that even in presence of high noise levels, the decision function is an efficient fault estimation indicator. When the noise level is high, the decision function and its slope are noisier. Conversely, the decision function and its slope are less noisy when the noise level is low. The results also show that for the three fault types under study (gain fault, phase shift fault, and mean value fault), the current components of the fictitious machines in the stationary frames have distinct robustness to noise.**

***Index Terms*—Fault severity estimation, 7-phase machines, Stationary frames, Noisy environment, CUSUM**

I. Introduction

Studies in the last decades, particularly monitoring of electrical machines, have provided important information on Fault Detection and Diagnosis (FDD), which is decomposed into fault detection, isolation and estimation [1]. Despite the continued dominance of three-phase machines, there is a growing trend towards designing and utilizing machines with five, seven, or nine phases, driven by their inherent ability to tolerate faults and distribute power more effectively [2], [3]. This paper will focus on a seven-phase electrical machine whose main application areas are air and sea transport or wind turbines.

The detection, isolation, and estimation of faults involve extracting and analyzing fault signatures or features from measured or estimated variables or parameters. The features can be extracted in the time, frequency, or time-frequency domain, depending on fault types. Reference [4] proposes a time-domain approach to detect and diagnose multiple faults in a three-phase electrical machine. Reference [5] introduced an analytical current flow model for a seven-phase machine and fault analysis performed in time and frequency domains.

The authors would like to thank China Scholarship Council for funding.

After the fault is detected and isolated, the estimation of its severity is crucial for maintenance and control reconfiguration. The estimator's performance depends on the accuracy of the estimation model and the quality of the measurements. Indeed, as the systems are increasingly complex, it is more challenging to develop accurate models [6], [7]. In [8], the authors designed an intermediate estimator to estimate the state and fault simultaneously by exploiting the properties of the fault distribution matrix. The authors in [9] developed a new real-time fault estimation module. This work is a follow up of [5] in which an analytical fault model is derived. The fault characteristics are processed through Cumulative Sum (CUSUM) algorithm. The slope of the decision function will be used as fault indicator. The performance of the fault estimation will be analyzed under noisy conditions and varying fault severities.

The contributions of this paper are:

1) Development of accurate analytical models in the stationary frames for phase currents, which are affected by faults that alter their amplitude, phase, or mean value.
2) Assessment of the fault severity estimation performance under various levels of noise and different fault types.

Fig. 1 describes the flowchart of the estimation procedure. The rest of this paper is structured as follows: Section II (right side of the flowchart) outlines the extraction of the theoretical relationship between fault severity and fault parameters in the absence of noise. Section III presents the CUSUM approach. Section IV explains how the fault severity is estimated from fault parameters under different noise levels, and estimation features also contained. In section V, the evaluation of the estimation performance, based on the analysis of the slope of the decision function from CUSUM algorithm, is provided in the different fictitious machines. The conclusions are given in section VI.

II. Noise-free phase currents analysis

A. Introduction

The currents in the 7-phase machine can be modeled using three representation spaces as an extension of the usual space vector definition used for 3-phase systems [3], [5], [10]:

- Natural frame: 7 phases denoted by variables i_1 to i_7.

979-8-3503-0014-7/23/$31.00 ©2023 IEEE
DOI 10.1109/PHM58589.2023.00053

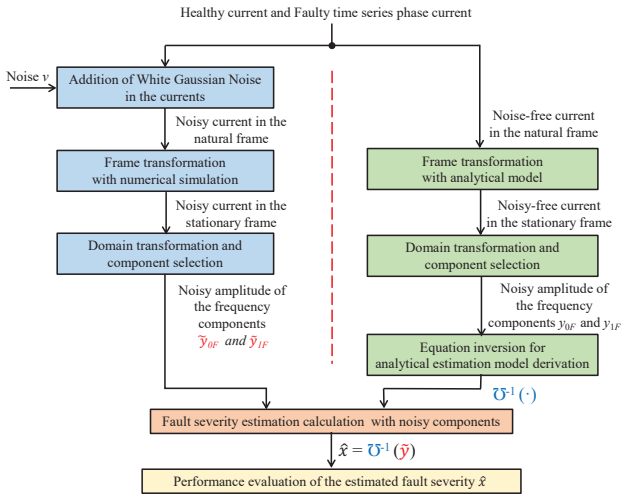

Fig. 1. Flowchart of fault estimation

- Stationary (α, β) frame: one-phase Homopolar Machine (HM) with variable i_0 with three two-phase independent fictitious machines, including a Principal Machine (PM) with $i_{p\alpha}$ and $i_{p\beta}$, a Secondary Machine (SM) with $i_{s\alpha}$ and $i_{s\beta}$, and a Tertiary Machine (TM) with $i_{t\alpha}$ and $i_{t\beta}$.
- Synchronous (d, q) frame: a one-phase HM and three $d-q$ orthogonal coordinate fictitious machines.

In this paper, the study is limited to the stationary space, and to the analysis of the DC component $(0F)$ and/or fundamental component $(1F)$ of the phase currents. The healthy and faulty currents in the natural frame are expressed as follows, respectively [5]:

$$i_{j(j=1...7)h} = I\sqrt{2}sin(\theta + (1-j)\varphi) \quad (1)$$

$$i_{j(j=1...7)f} = I\sqrt{2}(1+\triangle i_j)sin(\theta + (1-j)\varphi + \phi_j) + \gamma_j \quad (2)$$

where, $\theta = \omega t$, ω is the angular frequency; t is the current time; φ is the natural phase shift equals to $\frac{2\pi}{7}$ in the 7-phase machine; I is the RMS value of the phase current; $\triangle i_j$ will result in a gain fault, which is a modification of the current amplitude; ϕ_j will lead to a phase shift fault, which modifies the initial phase of the current; and γ_j, which represents a bias in the mean value of the current. The lower scripts h and f stand for the healthy and faulty conditions, respectively.

Equation (2) is used to simulate the different fault effects on phase currents.

B. Analytical model for fault severity estimation

By combining (2) with the Clarke transformation in (3), the analytical expressions of the phase currents in the stationary frames can be derived. The detailed derivation process can be found in [5].

Under healthy conditions, there is no current in the SM, TM, and HM. However, under faulty conditions, there are new components and/or frequency distortions in the actual phase currents. The frequency analysis is summarized in TABLE I. It can be observed that [5]:

1) The spectrum of the faulty current in the stationary frames includes DC $(0F)$ and/or fundamental component $(1F)$.
2) Only the mean value fault introduces a DC $(0F)$ component in the four fictitious machines.

TABLE I
FAULT FREQUENCIES IN THE STATIONARY FRAMES

Case	Current		Harmonic $0F$	Harmonic $1F$	Case	Current		Harmonic $0F$	Harmonic $1F$
H	PM	$i_{p\alpha}$		×	G	PM	$i_{p\alpha}$		×
		$i_{p\beta}$		×			$i_{p\beta}$		×
	SM	$i_{s\alpha}$				SM	$i_{s\alpha}$		×
		$i_{s\beta}$					$i_{s\beta}$		×(1)
	TM	$i_{t\alpha}$				TM	$i_{t\alpha}$		×
		$i_{t\beta}$					$i_{t\beta}$		×(1)
	HM	i_0				HM	i_0		×
PS	PM	$i_{p\alpha}$		×	MV	PM	$i_{p\alpha}$	×	×
		$i_{p\beta}$		×			$i_{p\beta}$	×(2)	×
	SM	$i_{s\alpha}$		×		SM	$i_{s\alpha}$	×	
		$i_{s\beta}$		×(1)			$i_{s\beta}$	×(3)	
	TM	$i_{t\alpha}$		×		TM	$i_{t\alpha}$	×	
		$i_{t\beta}$		×(1)			$i_{t\beta}$	×(3)	
	HM	i_0		×		HM	i_0	×	

H: healthy; G: gain fault; PS: phase shift fault; MV: mean value fault.
(1) For phase 1, no $1F$ component for $i_{s\beta}$ and $i_{t\beta}$.
(2) For phase 1, no $0F$ component for $i_{p\beta}$.
(3) For phase 1, no $0F$ component for $i_{s\beta}$ and $i_{t\beta}$.

The fault severity $x \in [0, 1]$ corresponds to the modification of parameters $\triangle i_j$, ϕ_j, and γ_j for gain, phase shift, and mean value faults, respectively. The function $y = \mho(x)$ expresses the relationship between the fault severity x and the amplitude of the components y for $0F$ and $1F$, as shown in TABLE II to TABLE IV. These functions, obtained noise-free conditions are then used to estimate the fault parameter from noisy faulty features (Fig. 1).

TABLE II
EVOLUTION OF FAULT SEVERITY UNDER GAIN FAULT

i	$0F$	$1F$
$i_{p\alpha}$	/	$y = \frac{1}{2} * \sqrt{\frac{1}{7}} * \sqrt{2x(x+7)(1+cos(j-1)2\varphi)+49} * I$
$i_{p\beta}$	/	$y = \frac{1}{2} * \sqrt{\frac{1}{7}} * \sqrt{2x(x+7)(1-cos(j-1)2\varphi)+49} * I$
$i_{s\alpha}$	/	$y = kx, \quad k = \frac{1}{2} * \sqrt{\frac{2}{7}} * \sqrt{1+cos(j-1)6\varphi} * I$
$i_{s\beta}$	/	$y = kx, \quad k = \frac{1}{2} * \sqrt{\frac{2}{7}} * \sqrt{1-cos(j-1)6\varphi} * I$
$i_{t\alpha}$	/	$y = kx, \quad k = \frac{1}{2} * \sqrt{\frac{2}{7}} * \sqrt{1+cos(j-1)4\varphi} * I$
$i_{t\beta}$	/	$y = kx, \quad k = \frac{1}{2} * \sqrt{\frac{2}{7}} * \sqrt{1-cos(j-1)4\varphi} * I$
i_0	/	$y = kx, \quad k = \frac{1}{2} * \sqrt{\frac{2}{7}} * I$

III. CUSUM ALGORITHM

The CUSUM algorithm was first proposed by Page in 1954 [11]. It is based on the sequential likelihood ratio analysis.

$$\begin{pmatrix} i_0 \\ i_{p\alpha} \\ i_{p\beta} \\ i_{t\alpha} \\ i_{t\beta} \\ i_{s\alpha} \\ i_{s\beta} \end{pmatrix} = \sqrt{\frac{2}{7}} \begin{pmatrix} \frac{1}{\sqrt{2}} & \frac{1}{\sqrt{2}} & \frac{1}{\sqrt{2}} & \frac{1}{\sqrt{2}} & \frac{1}{\sqrt{2}} & \frac{1}{\sqrt{2}} & \frac{1}{\sqrt{2}} \\ 1 & cos(\varphi) & cos(2\varphi) & cos(3\varphi) & cos(4\varphi) & cos(5\varphi) & cos(6\varphi) \\ 0 & sin(\varphi) & sin(2\varphi) & sin(3\varphi) & sin(4\varphi) & sin(5\varphi) & sin(6\varphi) \\ 1 & cos(2\varphi) & cos(4\varphi) & cos(6\varphi) & cos(8\varphi) & cos(10\varphi) & cos(12\varphi) \\ 0 & sin(2\varphi) & sin(4\varphi) & sin(6\varphi) & sin(8\varphi) & sin(10\varphi) & sin(12\varphi) \\ 1 & cos(3\varphi) & cos(6\varphi) & cos(9\varphi) & cos(12\varphi) & cos(15\varphi) & cos(18\varphi) \\ 0 & sin(3\varphi) & sin(6\varphi) & sin(9\varphi) & sin(12\varphi) & sin(15\varphi) & sin(18\varphi) \end{pmatrix} \begin{pmatrix} i_1 \\ i_2 \\ i_3 \\ i_4 \\ i_5 \\ i_6 \\ i_7 \end{pmatrix} \tag{3}$$

TABLE III
EVOLUTION OF FAULT SEVERITY UNDER PHASE SHIFT FAULT

i	$0F$	$1F$
$i_{p\alpha}$	/	$y = \frac{1}{2} * \sqrt{\frac{1}{7}} * \sqrt{39 + 10 * cos\varphi x - 10 * cos(j-1)2\varphi + 12 * cos(\varphi x - (j-1)2\varphi) - 2 * cos(\varphi x + (j-1)2\varphi)} * I$
$i_{p\beta}$	/	$y = \frac{1}{2} * \sqrt{\frac{1}{7}} * \sqrt{39 + 10 * cos\varphi x + 10 * cos(j-1)2\varphi - 12 * cos(\varphi x - (j-1)2\varphi) + 2 * cos(\varphi x + (j-1)2\varphi)} * I$
$i_{s\alpha}$	/	$y = \frac{1}{2} * \sqrt{\frac{1}{7}} * \sqrt{4 * (1 + cos(j-1)6\varphi - cos\varphi x) - 2 * (cos(\varphi x - (j-1)6\varphi) + cos(\varphi x + (j-1)6\varphi))} * I$
$i_{s\beta}$	/	$y = \frac{1}{2} * \sqrt{\frac{1}{7}} * \sqrt{4 * (1 - cos(j-1)6\varphi - cos\varphi x) + 2 * (cos(\varphi x - (j-1)6\varphi) + cos(\varphi x + (j-1)6\varphi))} * I$
$i_{t\alpha}$	/	$y = \frac{1}{2} * \sqrt{\frac{1}{7}} * \sqrt{4 * (1 + cos(j-1)4\varphi - cos\varphi x) - 2 * (cos(\varphi x - (j-1)4\varphi) + cos(\varphi x + (j-1)4\varphi))} * I$
$i_{t\beta}$	/	$y = \frac{1}{2} * \sqrt{\frac{1}{7}} * \sqrt{4 * (1 - cos(j-1)4\varphi - cos\varphi x) + 2 * (cos(\varphi x - (j-1)4\varphi) + cos(\varphi x + (j-1)4\varphi))} * I$
i_0	/	$y = \sqrt{\frac{1}{7}} * \sqrt{1 - cos\varphi x} * I$

TABLE IV
EVOLUTION OF FAULT SEVERITY UNDER MEAN VALUE FAULT

i	$0F$		$1F$
$i_{p\alpha}$	$y = kx,$	$k = 2 * \sqrt{\frac{1}{7}} * \lvert cos(j-1)\varphi) \rvert * I$	$y = \frac{\sqrt{7}}{2} * I$
$i_{p\beta}$	$y = kx,$	$k = 2 * \sqrt{\frac{1}{7}} * \lvert sin(j-1)\varphi) \rvert * I$	$y = \frac{\sqrt{7}}{2} * I$
$i_{s\alpha}$	$y = kx,$	$k = 2 * \sqrt{\frac{1}{7}} * \lvert cos(j-1)3\varphi) \rvert * I$	/
$i_{s\beta}$	$y = kx,$	$k = 2 * \sqrt{\frac{1}{7}} * \lvert sin(j-1)3\varphi) \rvert * I$	/
$i_{t\alpha}$	$y = kx,$	$k = 2 * \sqrt{\frac{1}{7}} * \lvert cos(j-1)2\varphi) \rvert * I$	/
$i_{t\beta}$	$y = kx,$	$k = 2 * \sqrt{\frac{1}{7}} * \lvert sin(j-1)2\varphi) \rvert * I$	/
i_0	$y = kx,$	$k = \sqrt{\frac{2}{7}} * I$	/

The idea is to accumulate information from the sampled data in such a way as to amplify any mismatch that may occur.

Let us assume n statistically independent samples of the vector $\widetilde{Y} = \{\widetilde{y}_k, k = 1, \cdots, n\}$. Each sample follows a probability distribution $p(\widetilde{y}_k, \vartheta)$ depending on a deterministic parameter ϑ. An abrupt change is modeled by an instantaneous modification of ϑ at the change time n_c. Before the change time n_c, $\vartheta = \vartheta_h$, and after the change time, $\vartheta = \vartheta_f$ [1]. A binary hypothesis is considered as follows:

$$\begin{aligned} &\text{under } H_0,\ \vartheta = \vartheta_h,\ 1 \le k \le n \\ &\text{under } H_1,\ \vartheta = \begin{cases} \vartheta_h,\ 1 \le k \le n_c \\ \vartheta_f,\ n_c + 1 \le k \le n \end{cases} \end{aligned} \tag{4}$$

The probabilities of $\widetilde{Y}$ under hypotheses H_0 and H_1 are:

$$\begin{aligned} p(\widetilde{Y}|H_0) &= \prod_{k=1}^{n} p(\widetilde{y}_k, \vartheta_h) \\ p(\widetilde{Y}|H_1) &= \prod_{k=1}^{n_c} p(\widetilde{y}_k, \vartheta_h) \prod_{k=n_c+1}^{n} p(\widetilde{y}_k, \vartheta_f) \end{aligned} \tag{5}$$

The deterministic parameter ϑ, can be the mean value μ or the variance σ^2 of a signal following a Gaussian distribution $\mathcal{N}(\mu, \sigma^2)$:

$$p(\widetilde{y}_k, \vartheta) = \frac{1}{\sqrt{2\pi\sigma^2}} \exp\left(-\frac{(\widetilde{y}_k - \mu)^2}{2\sigma^2}\right) \tag{6}$$

The Gaussian distribution $\mathcal{N}(\mu, \sigma^2)$ under two hypotheses are:

$$\begin{aligned} &H_0 :\ \widetilde{Y} = \{\widetilde{y}_k, k = 1, ..., n\} \backsim \mathcal{N}(\mu_h, \sigma_h^2) \\ &H_1 :\ \widetilde{Y} = \begin{cases} \widetilde{Y}_h = \{\widetilde{y}_k, k = 1, ..., n_c\} \backsim \mathcal{N}(\mu_h, \sigma_h^2) \\ \widetilde{Y}_f = \{\widetilde{y}_k, k = n_c + 1, ..., n\} \backsim \mathcal{N}(\mu_f, \sigma_f^2) \end{cases} \end{aligned} \tag{7}$$

Note that before the change time n_c, mean and variance are μ_h and σ_h^2, and after change time n_c, mean and variance are μ_f and σ_f^2.

The instantaneous log-likelihood ratio s_k at time k, which represents the difference between the log-likelihood of the observed data under two different hypotheses, is defined:

$$s_k = \ln(\frac{p(\widetilde{y}_k, \vartheta_f)}{p(\widetilde{y}_k, \vartheta_h)}) \tag{8}$$

Therefore combining (6) and (8), s_k can be calculated through the following expressions:

$$s_k = \ln \sigma_h - \ln \sigma_f + \frac{(\widetilde{y}_k - \mu_h)^2}{2\sigma_h^2} - \frac{(\widetilde{y}_k - \mu_f)^2}{2\sigma_f^2} \tag{9}$$

- if there is only mean change, $\sigma_h = \sigma_f$, it can be simplified:

$$s_k = \frac{\mu_f - \mu_h}{\sigma_h^2} \times (\widetilde{y}_k - \frac{\mu_f + \mu_h}{2}) \tag{10}$$

- if there is only variance change, $\mu_h = \mu_f$, it can be simplified:

$$s_k = \ln \sigma_h - \ln \sigma_f + (\frac{1}{\sigma_h^2} - \frac{1}{\sigma_f^2}) \times \frac{(\widetilde{y}_k - \mu_h)^2}{2} \tag{11}$$

The cumulative sum, used to compute the decision function in (13), is as follows:

$$S_n = \sum_{k=1}^{n} s_k \tag{12}$$

The decision function represents the deviation of the signal from a reference value over time. The decision function should stay close to zero if the signal is stable and does not change over time. However, if there is a change in the signal, such as a shift in the mean or the variance value, the decision function will follow a linear evolution whose slope is sensitive to the amplitude of the change.

$$G_n = S_n - \min_{1 \le n_c \le n} S_{n_c - 1} \tag{13}$$

IV. Noisy Phase Currents Analysis

A. Settings for the numerical model

A white Gaussian noise is added to the phase currents to simulate realistic measurements, and the noise level is defined by considering the Signal to Noise Ratio (SNR):

$$SNR = 10 \times \log_{10} \frac{\sigma_s^2}{\sigma_\upsilon^2} \tag{14}$$

where, σ_s^2 is the variance of the signal, and σ_υ^2 is the variance of the Gaussian distributed noise $\upsilon \sim \mathcal{N}(0, \sigma_\upsilon^2)$.

In the following simulations, the SNR is set to 20, 15, 10 and 5 dB, respectively. When the SNR decreases, the noise level increases. The fault levels are set to [5% to 30%] for the three cases, corresponding to gain fault $\triangle i_j$ varying from 0.05 to 0.3; phase shift fault ϕ_j varying from 0.05φ to 0.3φ; and mean value fault γ_j varying from $0.05I\sqrt{2}$ to $0.3I\sqrt{2}$. Two hundred simulations are run for the healthy conditions and for each faulty severity and noise level (three single fault types and four SNR values).

Without loss of generality, the RMS value of the phase current is set to 4A, and only the results for faults occurring in the fourth phase of the machine are presented.

B. Fault estimation features

The fault severity estimation under noisy conditions is performed in two steps:

1) The function $\mho^{-1}(\cdot)$ is obtained under noise-free conditions using the analytical models and the fault features (y, amplitude of DC and $1F$ components) and actual fault severity x.
2) The estimated the fault severity $\hat{x}$ is obtained from the fault amplitudes $\widetilde{y}$ extracted from noisy measurements, expressed as $\hat{x} = \mho^{-1}(\widetilde{y})$.

Fig. 2 shows the estimated fault severity plotted against the actual fault severity for gain fault case using $i_{p\alpha}$ under two different SNR levels, 20 dB and 5 dB. Each simulation (three single fault types and four SNR values) is repeated 200 times. The red dots represent the average values of the estimated. Indeed, they are found to be close to the actual fault level.

It can be also observed that the variance increases with the noise level and remains stable with increasing fault severity

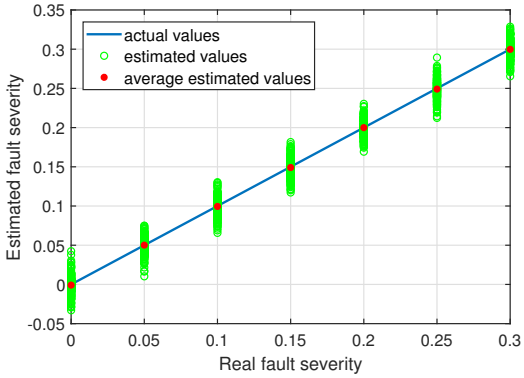

(a) SNR = 20 dB

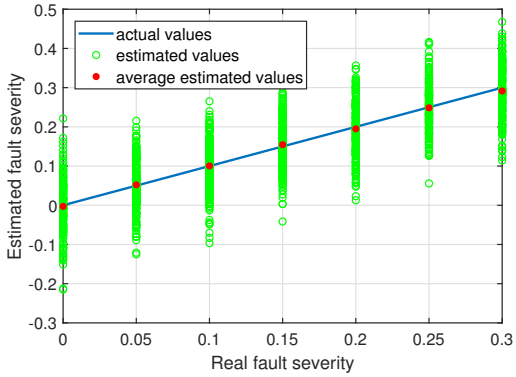

(b) SNR = 5 dB

Fig. 2. Fault severity estimation with $i_{p\alpha}$ under gain fault

as confirmed by the histograms displayed in Fig. 3. They show that the estimations follow a Gaussian distribution, as expected. Fig. 4 confirms the stable trend of the variance with increasing fault severity. The same computations are performed for all the components in stationary frames of the phase currents in the four fictitious machines.

V. Fault Estimation Evaluation

In the following, the first 200 samples represent the healthy cases, while the subsequent 200 ones stand for the faulty cases, as shown in Fig. 5.

The previous analysis showed that only the mean value is affected by the fault occurrence. The histograms in Fig. 3 also showed that we can assume the Gaussian distribution for the estimates. Therefore, the CUSUM algorithm can be applied using (10), (12), and (13) to measure the magnitude of the change in the signal and detect changes. Fig. 6 and Fig. 7 shows the results for 5% and 30% fault severity with $i_{p\alpha}$ under gain fault when SNR equals to 20 dB and 5 dB, respectively. The following conclusions can be drawn: the abrupt change in the fault estimate is clearly detected by the decision function, even if the noise level is high (SNR = 5 dB), and the slope of the decision function is sensitive to the fault severity.

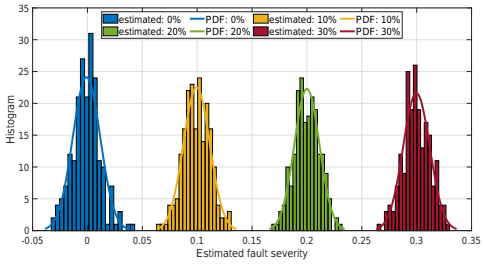

(a) SNR = 20 dB

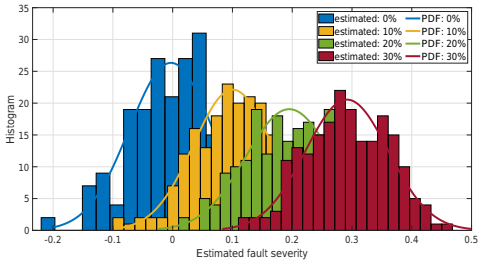

(b) SNR = 5 dB

Fig. 3. Histograms with $i_{p\alpha}$ under gain fault

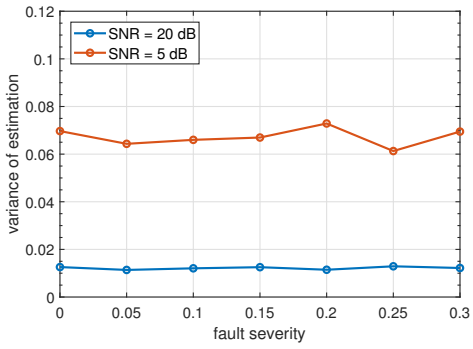

Fig. 4. Variance of the estimates with $i_{p\alpha}$ under gain fault

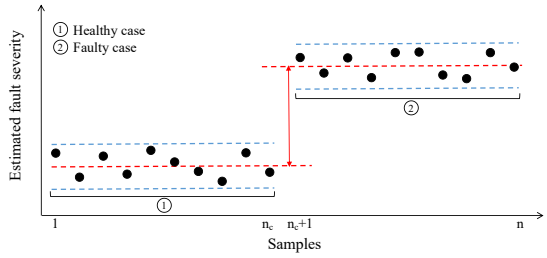

Fig. 5. Expected evolution of the sampled fault estimation severity

The slope's evolution along fault severity for different noise levels is plotted in Fig. 8 and Fig. 9. We can make the following comments:

1) The slope increases with the fault severity.
2) The difference in slope between two fault severities is more significant when the noise level is lower.
3) For the same noise level and fault severity, the slope for the three fault types is sorted as follows: mean value fault $>$ gain fault $>$ phase shift fault.
4) Particular attention need to be paid to $i_{p\alpha}$, $i_{p\beta}$ and $i_{s\alpha}$ components. For gain fault, $i_{p\beta}$ and $i_{s\alpha}$ are more sensitive to the noise; for phase shift fault, $i_{p\alpha}$, $i_{p\beta}$, and $i_{s\alpha}$ are more sensitive to the noise; and for mean value fault, $i_{p\beta}$ and $i_{s\alpha}$ are more sensitive to the noise.

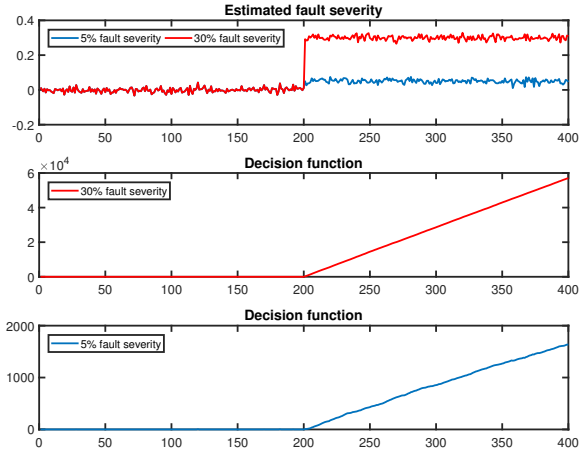

Fig. 6. Fault estimation and decision function with $i_{p\alpha}$ under gain fault and SNR = 20 dB

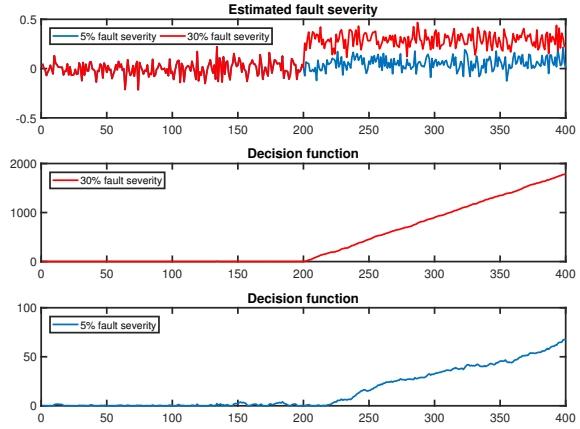

Fig. 7. Fault estimation and decision function with $i_{p\alpha}$ under gain fault and SNR = 5 dB

VI. Conclusion

This paper analyzed the performance of fault severity estimation under noisy conditions in a 7-phase electrical machine. The estimation model assumed that the faults affect the characteristics (amplitude, phase shift, and mean value) of the winding currents, whose components are derived in the stationary reference frames. The relationships between the fault severity and fault features (DC and $1F$ components) are

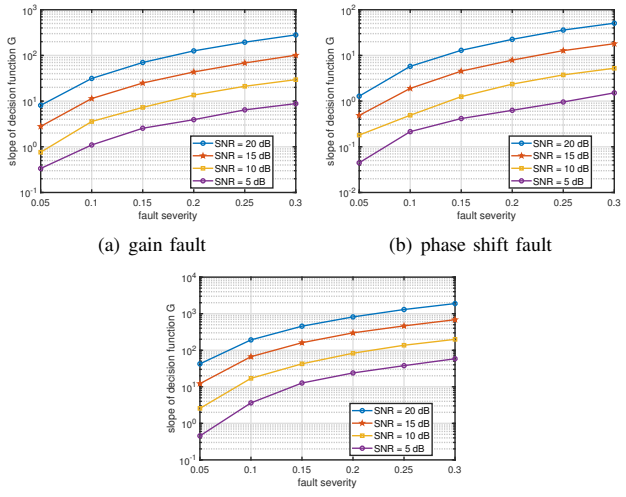

(a) gain fault (b) phase shift fault

(c) mean value fault

Fig. 8. CUSUM slope using $i_{p\alpha}$ for fault estimation

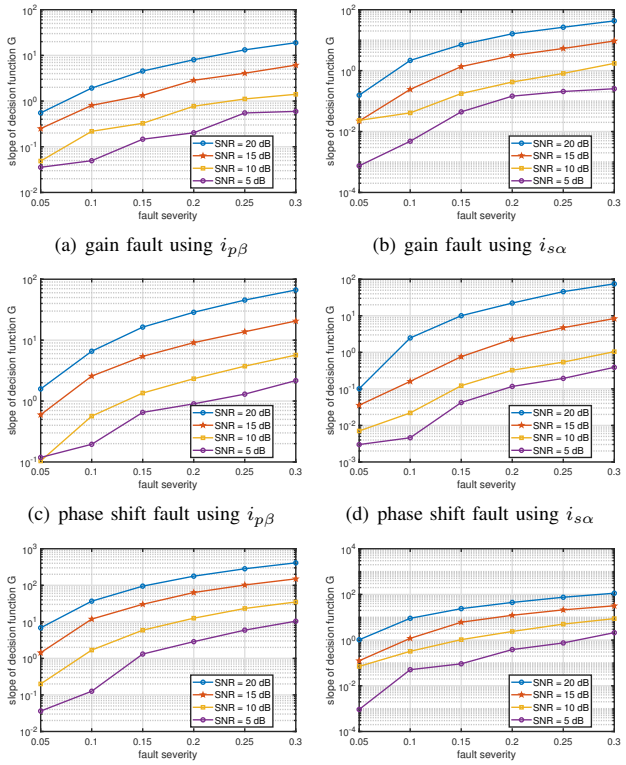

(a) gain fault using $i_{p\beta}$ (b) gain fault using $i_{s\alpha}$

(c) phase shift fault using $i_{p\beta}$ (d) phase shift fault using $i_{s\alpha}$

(e) mean value fault using $i_{p\beta}$ (f) mean value fault using $i_{s\alpha}$

Fig. 9. CUSUM slope for fault estimation

first extracted in noise-free conditions. These relations are then used to estimate the fault severities from noisy features. The performance of the estimation is evaluated with the CUSUM algorithm. Indeed, the simulation results for different fault severities (0 to 30%) and different noise levels (20 dB to 5 dB) showed that the decision function is an efficient fault indicator and that its slope is proportional to the fault severity. The results also show the sensitivity to noise depending on the components of the currents in the different fictitious machines used for fault severity estimation.

REFERENCES

[1] M. Basseville and I. V. Nikiforov, *Detection of abrupt changes: theory and application*. prentice Hall Englewood Cliffs, 1993, vol. 104.

[2] D. Diallo and C. Delpha, "Current-based analytical model derivation to analyse fault effects in 5-phase pmsm," in *2018 IEEE International Power Electronics and Application Conference and Exposition (PEAC)*. IEEE, 2018, pp. 1–6.

[3] E. Semail, A. Bouscayrol, and J.-P. Hautier, "Vectorial formalism for analysis and design of polyphase synchronous machines," *The European physical journal-applied physics*, vol. 22, no. 3, pp. 207–220, 2003.

[4] C. Delpha, D. Diallo, H. Al Samrout, and N. Moubayed, "Multiple incipient fault diagnosis in three-phase electrical systems using multivariate statistical signal processing," *Engineering Applications of Artificial Intelligence*, vol. 73, pp. 68–79, 2018.

[5] L. Zhang, C. Delpha, and D. Diallo, "Current-based analytical model for fault detection and diagnosis in 7-phase machines," in *IECON 2022–48th Annual Conference of the IEEE Industrial Electronics Society*. IEEE, 2022, pp. 1–6.

[6] S. M. Kay, *Fundamentals of statistical signal processing: estimation theory*. Prentice-Hall, Inc., 1993.

[7] J. Stoustrup and H. H. Niemann, "Fault estimation : a standard problem approach," *International Journal of Robust and Nonlinear Control: IFAC-Affiliated Journal*, vol. 12, no. 8, pp. 649–673, 2002.

[8] J.-W. Zhu, G.-H. Yang, H. Wang, and F. Wang, "Fault estimation for a class of nonlinear systems based on intermediate estimator," *IEEE Transactions on Automatic Control*, vol. 61, no. 9, pp. 2518–2524, 2015.

[9] B. Jiang and F. N. Chowdhury, "Fault estimation and accommodation for linear mimo discrete-time systems," *IEEE transactions on control systems technology*, vol. 13, no. 3, pp. 493–499, 2005.

[10] E. Semail, X. Kestelyn, and A. Bouscayrol, "Right harmonic spectrum for the back-electromotive force of an n-phase synchronous motor," in *Conference Record of the 2004 IEEE Industry Applications Conference, 2004. 39th IAS Annual Meeting.*, vol. 1. IEEE, 2004.

[11] E. S. Page, "Continuous inspection schemes," *Biometrika*, vol. 41, no. 1/2, pp. 100–115, 1954.